JACS Au
AN OPEN ACCESS JOURNAL OF THE AMERICAN CHEMICAL SOCIETY

pubs.acs.org/jacsau
Article

Photomediated Cationic Ring-Opening Polymerization of Cyclosiloxanes with Temporal Control

Wenxu Zhang,[‖] Shen Li,[‖] Shuting Liu, Tian-Tian Wang, Zheng-Hong Luo, Chao Bian,* and Yin-Ning Zhou*

Cite This: JACS Au 2024, 4, 4317−4327
Read Online
ACCESS | Metrics & More | Article Recommendations | Supporting Information

ABSTRACT: Precision synthesis of polyorganosiloxanes and temporal control over the polymerization process during ring-opening polymerization (ROP) of cyclosiloxanes remain challenging due to the occurrence of side reactions, e.g., intramolecular transfer (backbiting) and intermolecular chain transfer, and irreversible catalyst transformation. In this study, a merocyanine-based photoacid catalyst is developed for cationic ROP of different cyclosiloxanes. A series of well-defined cyclotrisiloxane polymers with predetermined molar masses and low dispersities ($Đ$ < 1.30) are successfully synthesized under various conditions (i.e., different catalyst loadings, initiator concentrations, solvents, and monomer types). Mechanistic insights by experiments and theoretical calculations suggest that the cationic active species, siloxonium ions, are combined with the catalyst anions to form tight ion pairs, thereby attenuating the reactivity of active species and subsequently minimizing side reactions. An efficient photocatalytic cycle is established among the catalyst, monomer, and polymer chain due to the rapid and reversible isomeric phototransformation of the catalyst, which endows the polymerization process with excellent temporal control. Successful in situ chain extension further confirms the controlled characteristics of photomediated CROP. This as-developed polymerization strategy effectively addresses long-standing challenges in the field of polyorganosiloxane synthesis.

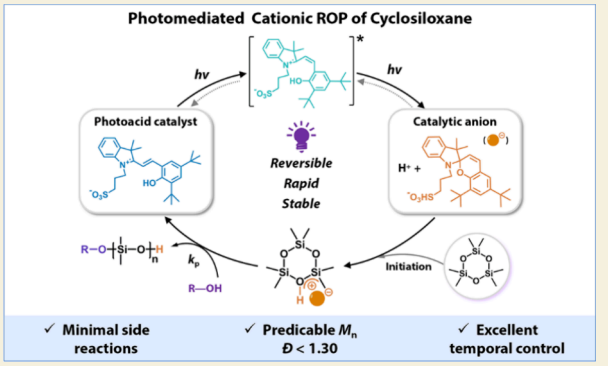

KEYWORDS: *photomediated cationic ROP, photoacid catalyst, polyorganosiloxanes, precision synthesis, temporal control*

INTRODUCTION

Siloxane-based polymeric materials have been widely applied in aerospace engineering, the automotive industry, electronic engineering, medical devices, and the construction industry because of their distinctive physical and chemical properties.[1−5] Polyorganosiloxanes are a class of hybrid organic/inorganic polymers characterized by the backbone consisting of alternating silicon and oxygen atoms, accompanied by organic groups in the side chain.[5−7] The commonly employed methods for synthesizing polyorganosiloxanes involve cationic ring-opening polymerization (CROP) of cyclosiloxanes with an acid catalytic system (e.g., Brønsted acids and Lewis acids) and anionic ring-opening polymerization (AROP) of cyclosiloxanes with a base catalytic system (e.g., alkali earth metal hydroxides, trisphosphazene organobase, and N-heterocyclic compounds).[8−11] Despite significant advancements in ROP methods, the precision synthesis of polyorganosiloxanes with predetermined molar masses and low dispersities is still challenging. Side reactions such as intramolecular transfer (backbiting) and intermolecular chain transfer occur during the polymerization, leading to an equilibrium with chain propagation and thus interior control over chain microstructures, given the formation of byproducts such as cyclic siloxanes and linear oligomers.

Several research groups have made efforts to achieve the precision synthesis of polyorganosiloxanes by carefully selecting appropriate initiators, catalysts, and reaction conditions. Li and co-workers developed a strategy for achieving the controlled AROP to yield well-defined polyorganosiloxanes using trisphosphazene base as the catalyst and benzyl alcohol as the initiator at room temperature.[12,13] Fuchise and co-workers conducted a series of works on organocatalytic living AROP of functionalized cyclotrisiloxanes using amidines or guanidines as catalysts and water or silanols as initiators.[14−20] However, it should be noted that all the aforementioned systems proceed based on the AROP mechanism.

Alternatively, the development of controlled CROP techniques is still lacking despite its potential applicability to

Received: July 29, 2024
Revised: September 11, 2024
Accepted: September 13, 2024
Published: September 25, 2024

https://doi.org/10.1021/jacsau.4c00682
JACS Au 2024, 4, 4317−4327

a wider range of monomers (i.e., functional cyclosiloxanes with a silicon−hydrogen or silicon−chlorine bond that are not stable in the presence of strong bases). In this regard, some researchers found that trisiloxonium ions, as the cationic active species generated during chain initiation and propagation, possess high reactivity that may result in intramolecular transfer (backbiting) and intermolecular chain transfer reactions.[21−23] To achieve controlled CROP, it is crucial to reduce the reactivity of cationic active species.[24−26] Taking inspiration from the previous work on controlled AROP reported by Kato and co-workers,[27] anion active species were transformed into tight ion pairs through combination with the phosphorus catalyst cations. This process enhances the steric hindrance of the active species to reduce its nucleophilic attack reactivity, thereby preventing intramolecular transfer (backbiting) and intermolecular chain transfer reactions. Hopefully, the use of a catalyst that can generate effective catalytic anions to form tight ion pairs with cationic active species is highly desirable to minimize side reactions and achieve the controlled CROP of cyclic siloxanes.

Furthermore, precise control over the structure and function of polymers has recently aroused interest by using temporally controlled polymerizations, which has not been achieved yet during the ROP of cyclosiloxanes. The use of external stimuli,[28,29] such as light,[30−32] electricity,[33−37] and mechanical force,[38−41] provides temporal control over polymerization by modulating the catalytic activity. Among these stimuli, light attracts more attention due to its advantages of facile operation, noninvasiveness, and exceptional spatial and temporal control.[42−47] In a light-switchable polymerization system, it is crucial that the photocatalysts exhibit complete reversibility while ensuring rapid and quantitative switching of the propagating chain between an active state and a dormant state upon light being turned on and off. Although benzophenone and sulfonium have been utilized as photocatalysts for photoinitiated CROP of cyclosiloxanes,[48,49] these polymerizations fail to achieve temporal control due to the irreversible transformation of catalysts.

In this work, we develop an unprecedented photomediated CROP strategy to synthesize well-defined polyorganosiloxanes with significantly suppressed side reactions and excellent temporal control by using a newly designed merocyanine-based photoacid catalyst. Detailed mechanistic investigations are carried out through synergetic experiments and density functional theory (DFT) calculations. Kinetic characteristics of photomediated CROP are illustrated under different conditions including different catalyst loadings, initiator concentrations, solvents, and monomer variations. Light on−off switching experiments and in situ chain extension experiments are performed to evaluate temporal control capability and chain-end fidelity, respectively. This newly developed polymerization strategy enables precise and temporal control over the polymerization of cyclosiloxanes and thus makes great advances in the field of polyorganosiloxane synthesis.

EXPERIMENTAL SECTION

Materials

1,3-Propane sultone ($C_3H_6O_3S$, Bidepharm, 98%), 2,3,3-trimethylindolenine ($C_{11}H_{13}N$, Bidepharm, 98%), salicylaldehyde ($C_7H_6O_2$, Adamas, 99%), 3,5-di-*tert*-butylsalicylaldehyde ($C_{15}H_{22}O_2$, Adamas, 98%+), hexamethylcyclotrisiloxane (D_3, Adamas, 98%+), 2,4,6,8-tetramethylcyclotetrasiloxane (D_4H, Adamas, 98%+), 1,3,5-trivinyl-1,3,5-trimethylcyclotrisiloxane (D_3^{Vi}, Adamas, 95%+), 1,3,5-trimethyl-1,3,5-tris(3,3,3-trifluoropropyl)cyclotrisiloxane (D_3^{TFPr}, Adamas, 98%+), 1,3,5-trimethyl-1,3,5-triphenylcyclotrisiloxane (D_3^{Ph}, Adamas, 97%), benzyl alcohol (BnOH, Adamas, 99%), trifluoromethanesulfonic acid (CF_3SO_3H, Adamas, 99%+), toluene (C_7H_8, Adamas, 99.8%), tetrahydrofuran (THF, Adamas, 99.9%), 1,4-dioxane ($C_4H_8O_2$, Adamas, 99.7%), chloroform (CH_3Cl, Adamas, 99.9%), cyclohexane (C_6H_{12}, Adamas, 99.0%), ethanol (EtOH, Greagent, 99.7%+), acetonitrile (MeCN, Adamas, 99.9%), and diethyl ether (CH_3OCH_3, Sinopharm, 99.7%+) were used as received.

Instrumentation

^1H and ^{13}C nuclear magnetic resonance (NMR) spectra were acquired on a Bruker Avance III HD 400 MHz spectrometer. Monomer conversions were determined by analyzing the ^1H NMR spectra of the polymerization product. Number-average molar mass (M_n), mass-average molar mass (M_w), and dispersity ($Đ = M_w/M_n$) of the resulting polymers were detected by gel permeation chromatography (1260 Infinity II GPC, Agilent) with the PLgel Mixed-C column (7.5 mm × 300 mm, 5 μm particle size), using toluene as an eluent at a flow rate of 1 mL/min at 40 °C. Linear polystyrenes with low dispersity (M_n ranging from 1000 to 1×10^6 g/mol and $Đ$ ranging from 1.02 to 1.08) were used as reference standards for calibration purposes. UV−visible absorption spectra of the synthesized photocatalyst were measured with a Lengguang Technology UV7600 UV/vis spectrometer in toluene. pH values of the solution of the synthesized photocatalyst in toluene were recorded using a Shanghai Leici PHSJ-5T pH meter with potassium hydrogen phthalate aqueous solution (pH 4.00) and potassium dihydrogen phosphate aqueous solution (pH 6.86) as reference standards. The polymerizations were conducted in a Shanghai Titan PR-6 photochemical reactor equipped with a blue LED light source emitting at $\lambda_{max} \approx 460−465$ nm and an intensity of 8 W while maintaining a reaction temperature of 30 °C.

Synthesis of the Merocyanine-Based Photoacid Catalyst

A mixture of 2,3,3-trimethylindole (1.65 g, 0.01 mol) and 1,3-propanesulfonate (1.26 g, 0.01 mol) was placed in a 50 mL Schlenk flask equipped with a magnetic stirrer. The reaction mixture was heated to 90 °C in an oil bath under a nitrogen atmosphere and stirred for 4 h. After completion of the reaction, the resulting mixture was washed with cold ether and filtered to obtain 2,3,3-trimethyl-1-(3-sulfopropyl)-3H-indolium. The product was dried in a vacuum drying oven and collected as a purple solid (2.55 g, 87% yield). The reaction scheme is shown in Scheme S1. The ^1H NMR spectrum of the obtained compound is shown in Figure S1.

2,3,3-Trimethyl-1-(3-sulfopropyl)-3H-indolium (500 mg, 1.8 mmol) was dissolved in 10 mL of anhydrous ethanol and placed in a 50 mL round-bottomed flask. Subsequently, 2-hydroxybenzaldehyde (240 mg, 1.95 mmol) was added to the mixture, which was then transferred into an oil bath at a temperature of 90 °C with continuous reflux stirring for a duration of 16 h. After the reaction mixture was cooled in a refrigerator, the resulting product was collected through vacuum filtration. The obtained powder was washed with excess *n*-hexane and dried under vacuum conditions at a constant temperature of 120 °C until reaching a constant weight. Finally, the orange powder 2-(2-hydroxystyryl)-3,3-dimethyl-1-(3-sulfopropyl)-3H-indolium (PAG1, 533.4 mg, 77.6%) was obtained. The reaction scheme is shown in Scheme S2. The ^1H NMR and ^{13}C NMR spectra of PAG1 are shown in Figures S2 and S3, respectively.

A modified merocyanine-based photoacid catalyst 2-(3,5-di-*tert*-butyl-2-hydroxystyryl)-3,3-dimethyl-1-(3-sulfopropyl)-3H-indolium (PAG2) was synthesized according to the same procedure using 2,3,3-trimethyl-1-(3-sulfopropyl)-3H-indol (1.65 g, 0.01 mol) and 3,5-di-*tert*-butyl-2-hydroxybenzaldehyde (1.26 g, 0.01 mol) as the reactants. Finally, the bright orange powder PAG2 (533.4 mg, 77.6%) was obtained. The reaction scheme is shown in Scheme S3. The ^1H NMR and ^{13}C NMR spectra of PAG2 are shown in Figures S4 and S5, respectively.

General Procedure for Photo-CROP of Cyclosiloxanes

In a typical procedure, D_3 (1.779 g, 7.9 mmol), PAG2 (0.0199 g, 0.04 mmol), BnOH (8.3 mL, 0.079 mmol), and 5 mL of toluene were

https://doi.org/10.1021/jacsau.4c00682
JACS Au 2024, 4, 4317−4327

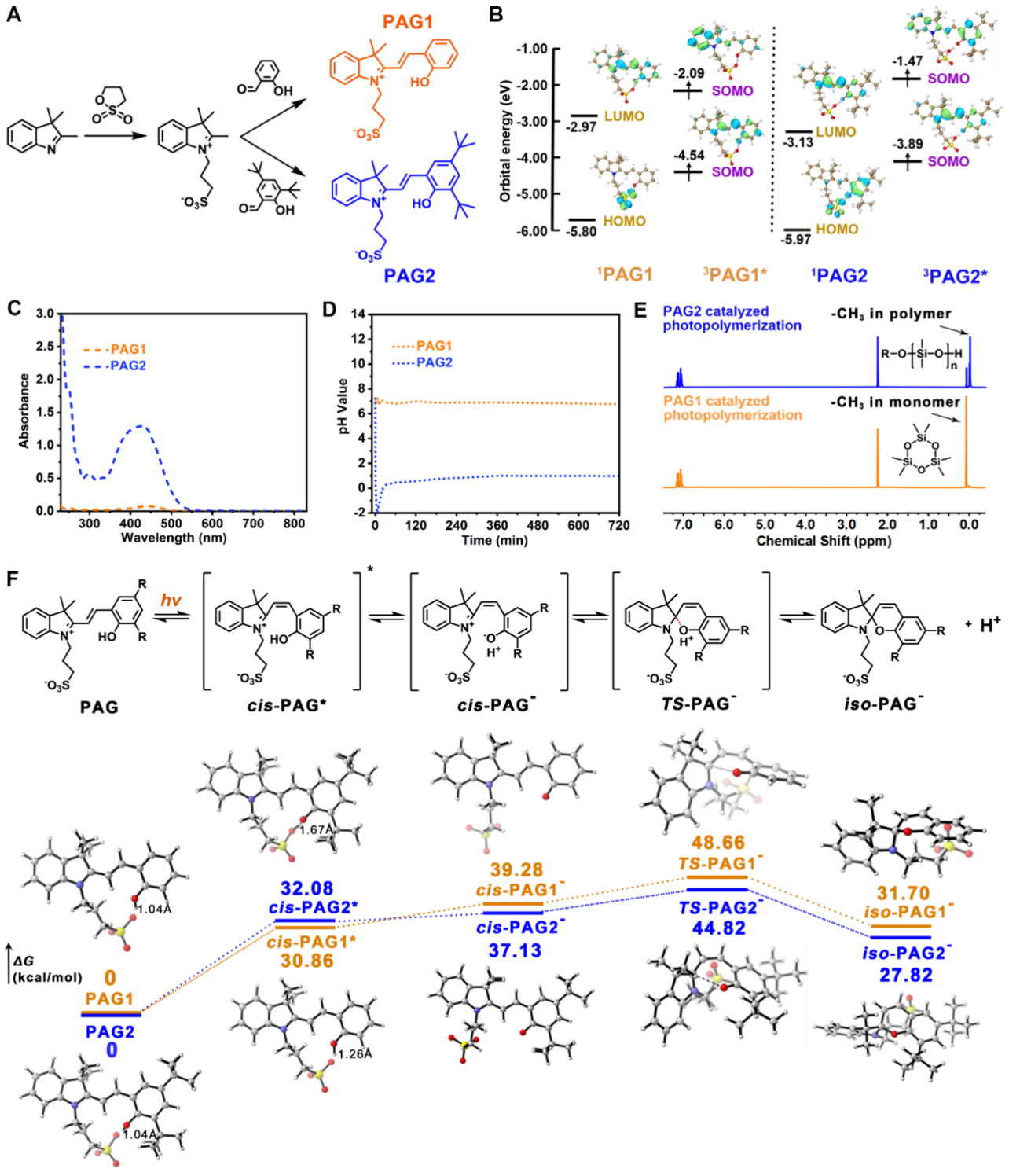

Figure 1. (A) Synthetic route, (B) DFT calculations of orbitals, (C) UV−vis spectra of PBG1 (0.26 mmol/L) and PBG2 (0.20 mmol/L) in toluene, (D) pH value of PBG1 (8 mmol/L) and PBG2 (8 mmol/L) in toluene under 460−465 nm light irradiation (8 W), (E) ^{1}H NMR of the products under the photopolymerization condition of $[D_3]_0/[BnOH]_0/[PAG]_0$ = 100:1:0.5 in toluene under 460−465 nm light irradiation (8 W), and (F) energy profiles of PAG during the process of photomediated reversible isomeric transformation.

sequentially introduced into a 25 mL Schlenk flask. The flask was hermetically sealed with a rubber stopper and purged of oxygen through three freeze−pump−thaw cycles. Subsequently, the polymerization reaction was conducted in a photochemical reactor at 30 °C. Samples were extracted at predetermined time intervals using a syringe for ^{1}H NMR and GPC analyses. The resulting polymer was obtained by precipitating the reaction mixture in cold methanol to remove the residual monomer and the catalyst. Polymerizations under different conditions follow the same protocol. The stability of the resulting polymers upon storage at room temperature has been confirmed by the unchanged average molar mass (Table S1).

In Situ Chain Extension

The macroinitiator polydimethylsiloxane (PDMS) was synthesized via photo-CROP of D_3 under the conditions $[D_3]_0/[BnOH]_0/[PAG2]_0$ = 100/1/0.5, $[D_3]_0$ = 1.58 mol/L in toluene, following the

https://doi.org/10.1021/jacsau.4c00682
JACS Au 2024, 4, 4317−4327

Table 1. Photomediated CROP of D_3 under Various Conditions

entry[a]	$[M]_0/[initiator]_0/[cat]_0$	time (h)	conversion (%)[f]	$M_{n,th}$[g]	$M_{n,GPC}$[h]	$Đ$ (M_w/M_n)[h]
1[b]	100/1/0.5	12				
2	100/1/0	12				
3	100/1/0.25	12	75.5	16,902	17,100	1.23
4	100/1/0.5	12	91.3	20,415	19,200	1.27
5	100/1/1	12	97.9	21,894	20,700	1.25
6	100/2/0.5	12	93.6	10,522	9200	1.18
7	100/0.67/0.5	12	90.4	30,290	25,600	1.29
8[c]	100/1/0.5	12	85.4	19,100	17,900	1.19
9[d]	100/1/0.5	12	96.4	21,553	18,300	1.48
10[e]	100/1/0.5	4	>99.9	22,354	14,900	2.56

[a]Polymerization conditions: $[D_3]_0$ = 1.58 mol/L in toluene under blue light irradiation (460−465 nm, 8 W) at 30 °C using benzyl alcohol (BnOH) as the initiator and PAG2 as the catalyst. [b]Polymerization without light irradiation. [c]Polymerization in cyclohexane. [d]Polymerization in chloroform. [e]Polymerization without light irradiation at 30 °C using BnOH as the initiator and CF_3SO_3H as the catalyst. [f]Monomer conversions were calculated by ^1H NMR. [g]$M_{n,th} = [M]_0/[initiator]_0 \times conversion + M_{initiator}$. [h]Determined by GPC in toluene.

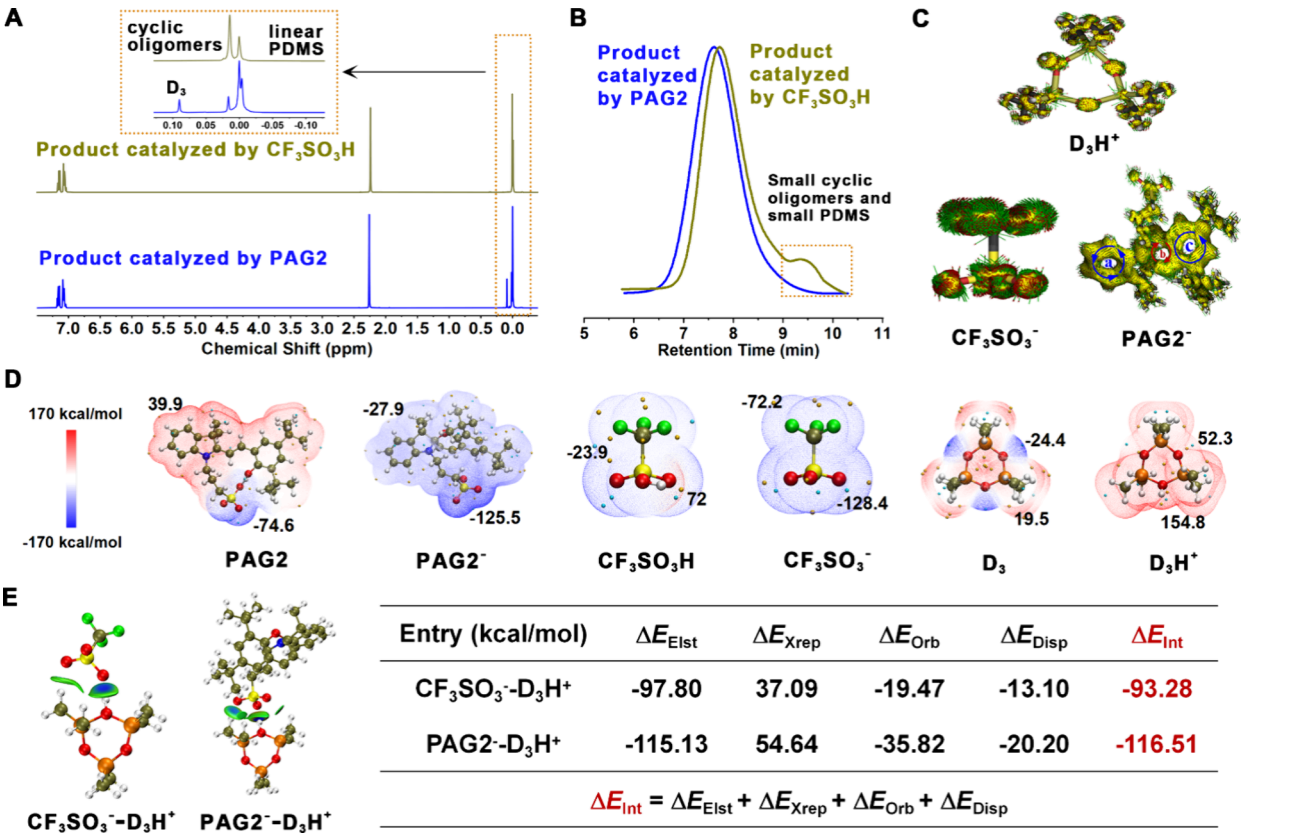

Entry (kcal/mol)	ΔE_{Elst}	ΔE_{Xrep}	ΔE_{Orb}	ΔE_{Disp}	ΔE_{Int}
$CF_3SO_3^-$-D_3H^+	-97.80	37.09	-19.47	-13.10	-93.28
PAG2$^-$-D_3H^+	-115.13	54.64	-35.82	-20.20	-116.51

$$\Delta E_{Int} = \Delta E_{Elst} + \Delta E_{Xrep} + \Delta E_{Orb} + \Delta E_{Disp}$$

Figure 2. (A) ^1H NMR spectra of the photopolymerization products; (B) GPC curves of the photopolymerization products; (C) anisotropy of the induced current density (AICD) of proton transfer products D_3H^+, $CF_3SO_3^-$, and PAG2$^-$; (D) electrostatic potential (ESP) of PAG2, PAG2$^-$, CF_3SO_3H, $CF_3SO_3^-$, D_3, and D_3H^+; and (E) interaction energies (ΔE_{Int}) of ion pairs PAG2$^-$−D_3H^+ and $CF_3SO_3^-$−D_3H^+ via DFT calculations.

aforementioned procedure. After 12 h, a degassed mixture of the D_3 monomer and toluene was added for chain extension using a nitrogen-purged syringe, and the resulting mixture continued to react in a photochemical reactor for 6 h before samples were taken for analysis.

RESULTS AND DISCUSSION

Synthesis of the Merocyanine-Based Photoacid Catalyst

The merocyanine-based photoacid catalyst 2-(2-hydroxystyryl)-3,3-dimethyl-1-(3-sulfopropyl)-3H-indolium (PAG1) has been developed for precise control of the photopolymerization of cyclic lactones.[50,51] However, our preliminary attempt at the photopolymerization of cyclotrisiloxanes by using PAG1 failed, which can be attributed to its limited solubility in aprotic organic media (e.g., toluene, THF, and 1,4-dioxane), further leading to inadequate release of hydrogen ions. Moreover, a relatively higher silicon−oxygen bond energy compared to organic C−O−C linkages in cyclic ester requires a stronger acidic condition to initiate ROP.[52] One effective way to improve the solubility of PAG1 in organic media is the introduction of alkyl groups. Bearing these considerations in mind, a photoacid catalyst 2-(3,5-di-*tert*-butyl-2-hydroxystyryl)-3,3-dimethyl-1-(3-sulfopropyl)-3H-indolium (PAG2) is designed and synthesized via the introduction of two *tert*-butyl groups on the phenol moiety, as depicted in Figure 1A.

https://doi.org/10.1021/jacsau.4c00682
JACS Au 2024, 4, 4317−4327

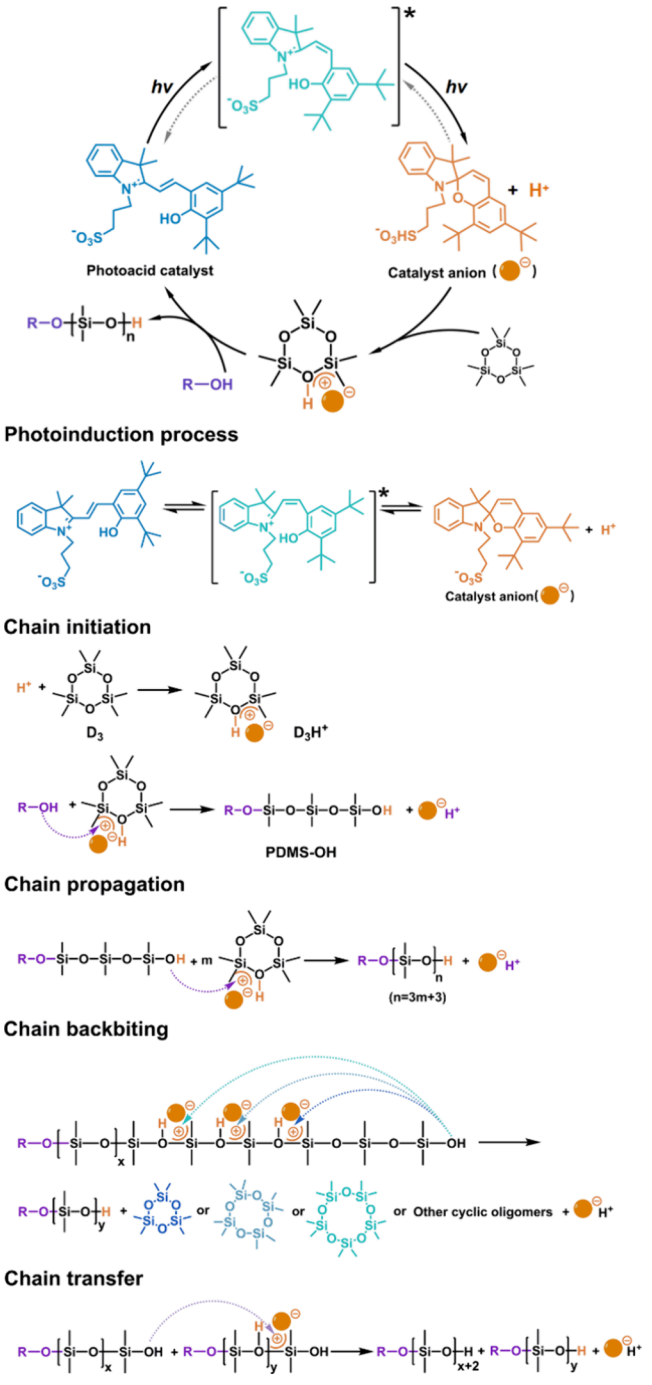

Figure 3. Mechanism of photomediated CROP of D_3.

The lowest unoccupied molecular orbitals (LUMO) and the highest occupied molecular orbitals (HOMO) of the ground-state catalysts PAG1 and PAG2, as well as the singly occupied molecular orbitals (SOMO) of the excited-state catalysts PAG1* and PAG2*, along with their corresponding energy levels, were calculated by time-dependent DFT (TD-DFT) calculations in Gaussian 16 using the PBE0 method and the 6-311G(d,p) basis set (details can be found in the Supporting Information). As shown in Figure 1B, a decrease in both HOMO and LUMO energies is observed for PAG2 compared to PAG1. Furthermore, the HOMO of PAG1 is found to be localized on the sulfonic moiety, whereas the HOMO of PAG2 exhibits distribution across both sulfonic and phenol moieties, confirming a change in the planar conjugated structure due to the incorporation of *tert*-butyl groups. The SOMO energy of PAG2* is higher than that of PAG1*, indicating an increased activity in the excited state and a higher potential to participate in chemical reactions.

The photochemical properties of PAG1 and PAG2 in toluene were evaluated. As shown in Figure 1C, the molar absorption coefficient ($\varepsilon_{max,abs}$ = 9715 L mol^{-1} cm^{-1}) of PAG2 at the maximum wavelength of absorption ($\lambda_{max,abs}$ = 428 nm) in toluene is higher than that of PAG1 ($\varepsilon_{max,abs}$ = 431 L mol^{-1} cm^{-1} at $\lambda_{max,abs}$ = 443 nm). Additionally, under 460 nm LED light irradiation in toluene (Figure 1D), PAG2 shows a lower pH value (pH ≈ 1.0) compared to PAG1 (pH ≈ 6.9) after a 30 min stabilization. These results suggest that PAG2 possesses superior photochemical performance and greater hydrogen ion release capacity due to enhanced solubility in toluene. The polymerization of hexamethylcyclotrisiloxane (D_3) was performed using PAG1 and PAG2 as catalysts under light irradiation in toluene, respectively (Figure 1E). No polymerization occurred with PAG1 as the catalyst, whereas the polymerization with PAG2 achieved a monomer conversion of 91.3% after 12 h of light irradiation, indicating the successful development of the catalyst.

Another crucial characteristic of the merocyanine-based photoacid catalyst (PAG) is its ability to undergo rapid and reversible isomeric transformation under light irradiation, which enables temporal control in photopolymerizations. The process of reversible isomeric transformation from the reactant (PAG) to the product (*iso*-PAG) involves three catalyst intermediates (i.e., *cis*-PAG*, *cis*-PAG$^-$, and *TS*-PAG$^-$).[53,54] Herein, a relatively stable species of *iso*-PAG is detected by ^{1}H NMR as shown in Figure S6, while *cis*-PAG2*, *cis*-PAG2$^-$, and *TS*-PAG2$^-$ are not detected. Additionally, free energies of the reactants, intermediates, and products for PAG1 and PAG2 were calculated by DFT calculations combined with the quasi-rigid-rotor harmonic oscillator (q-RRHO) model, the solvation model based on the density (SMD) model, and the frequency correction factor, and the energy profiles are illustrated in Figure 1F. The energy levels of *cis*-PAG2$^-$ (37.13 kcal/mol) and *TS*-PAG2$^-$ (44.82 kcal/mol) are found to be lower than those of *cis*-PAG1$^-$ (39.28 kcal/mol) and *TS*-PAG1$^-$ (48.66 kcal/mol), respectively, indicating that the energy barriers for reversible isomeric transformation after the photoexcitation process in PAG2 are smaller than those in PAG1. Furthermore, the higher energy level of *cis*-PAG2* (32.08 kcal/mol) and the lower energy level of *iso*-PAG2$^-$ (27.82 kcal/mol), compared to *cis*-PAG1* (30.86 kcal/mol) and *iso*-PAG1$^-$ (31.70 kcal/mol), suggest an enhanced reactivity after photoexcitation and an increased stability of the products. All the computational results support that PAG2 displays superior photocatalytic activity and exhibits a faster reversible isomeric transformation.

The synthesized PAG2 was further evaluated by conducting polymerizations of D_3 under various conditions including different PAG2 loadings, initiator concentrations, and solvents. The corresponding results are listed in Table 1. The absence of light irradiation or PAG2 (entries 1 and 2) results in no polymerization, highlighting the indispensability of both components. Controlled polymerizations of D_3 are achieved in toluene with various loadings of PAG2 at the molar ratios of 100:0.25, 100:0.5, and 100:1 versus monomer concentration (entries 3, 4, and 5) and different targeted degrees of polymerization (DP) of 50, 100, and 150 (entries 3, 6, and

https://doi.org/10.1021/jacsau.4c00682
JACS Au 2024, 4, 4317−4327

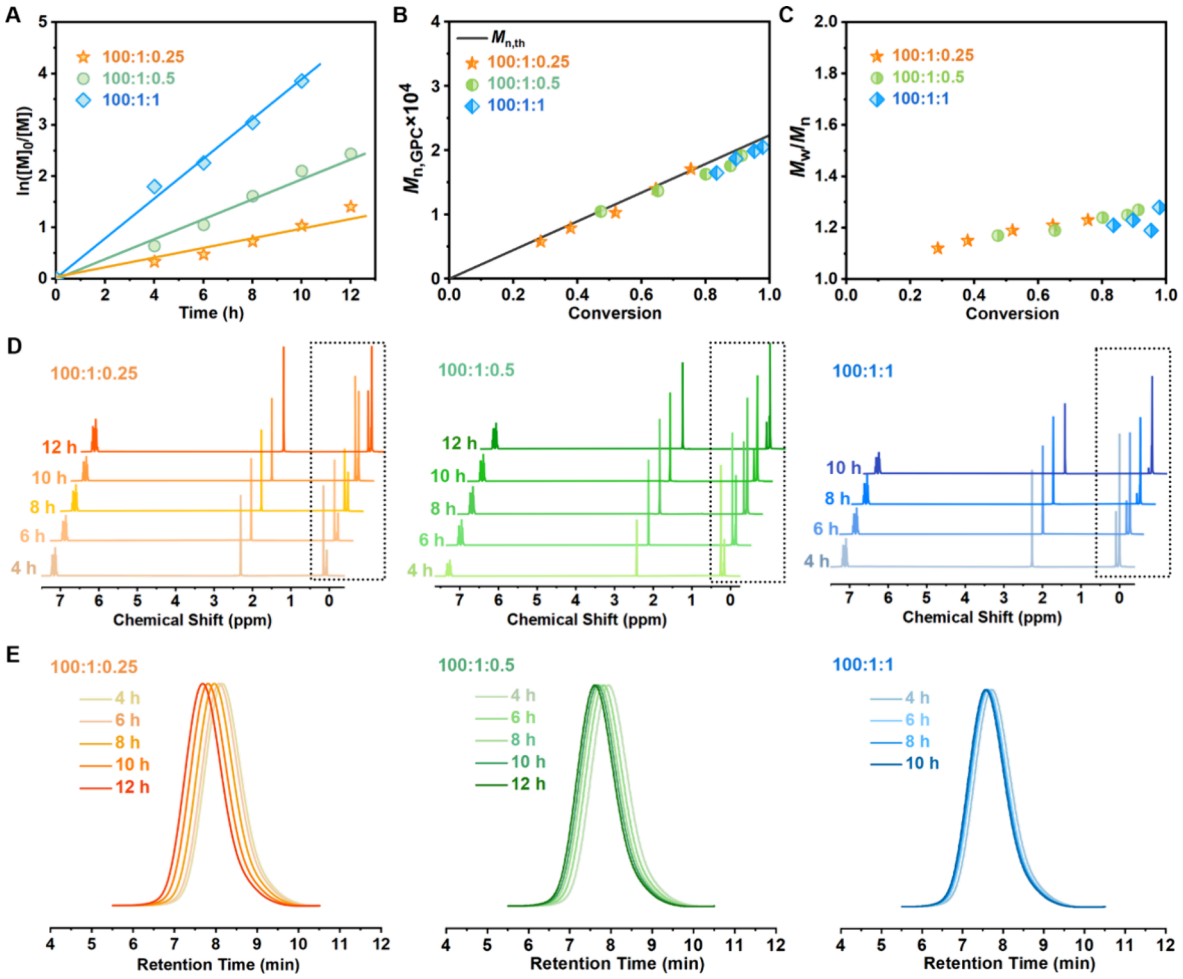

Figure 4. Polymerization kinetics via photomediated CROP of D_3 under different PAG2 loadings: (A) semilogarithmic kinetic plots versus time, (B) evolution of M_n versus conversion, (C) evolution of $Đ$ (M_w/M_n) versus conversion, (D) ^{1}H NMR spectra of the products, and (E) GPC curves of the resulting polymers.

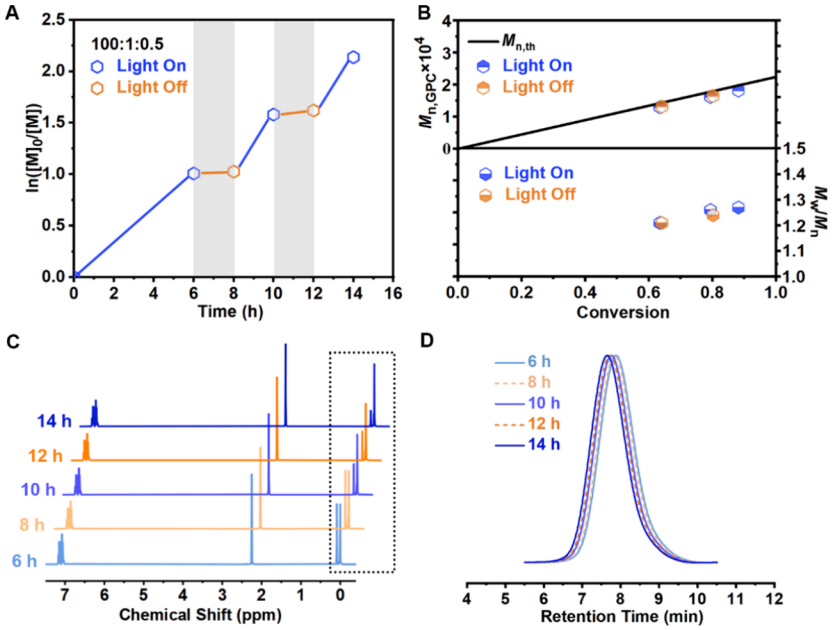

Figure 5. Temporal control of photomediated CROP of D_3 by switching the light on−off: (A) semilogarithmic kinetic plots versus time, (B) evolution of M_n and $Đ$ (M_w/M_n) versus conversion, (C) ^{1}H NMR spectra of the products, and (D) GPC curves of the resulting polymers.

https://doi.org/10.1021/jacsau.4c00682
JACS Au 2024, 4, 4317−4327

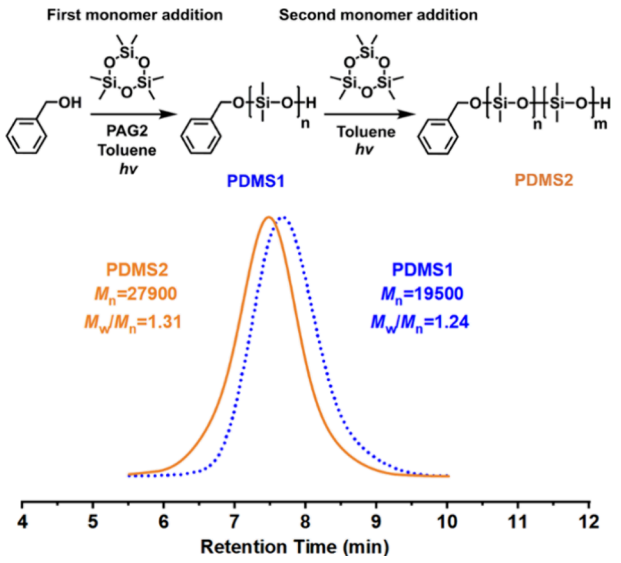

Figure 6. In situ chain extension and GPC curves of the resulting polymers.

7). The resulting polymers (PDMS) exhibit low dispersities ($Đ$ = 1.18−1.29) and predetermined molecular masses. An increased loading of PAG2 leads to an enhanced polymerization rate due to the higher concentration of hydrogen ions released, while a decrease in initiator concentration results in an increased molar mass because of a lower number of propagating chains.

Various solvents, including cyclohexane (dielectric constant ε = 0.1) and chloroform (ε = 4.4), were employed for the polymerization of D_3 with PAG2 in entries 8 and 9. In comparison to the polymerization conducted in toluene (ε = 2.4), monomer conversion after 12 h decreases from 91.3 to 85.4%, suggesting that the solvent with a lower dielectric constant (e.g., cyclohexane) results in a diminished polymerization rate. The solvent chloroform with a higher dielectric constant enables a faster polymerization, but the product yielded has a higher dispersity of 1.48. Consequently, toluene is considered as a promising solvent for the polymerization. The underlying mechanisms governing controlled polymerizations of D_3 using PAG2 as a catalyst, along with the influence of the solvent on cationic polymerizations, are discussed in detail below.

Mechanistic Insights

The cationic polymerization of D_3, as suggested by previous reports,[21−23] involves the generation of trisiloxonium ions through the combination of protonic hydrogen (H^+). Subsequently, a protonic initiator attacks and cleaves the Si−O bond to form a polymer chain. Due to the high activity of trisiloxonium ions, side reactions such as intramolecular transfer (backbiting) and intermolecular chain transfer easily occur, thereby impeding precise control over the polymerization. However, in the photopolymerizations of D_3 with PAG2, catalyst anions $PAG2^-$ are generated to form ion pairs ($PAG2^-$−D_3H^+) with trisiloxonium ions, which reduces the activity of active species and minimizes side reactions. To further understand the effect of ion pairs, a controlled experiment using conventional trifluoromethanesulfonic acid (CF_3SO_3H) as an acid catalyst was proceeded (entry 10, Table 1), in which ion pairs $CF_3SO_3^-$−D_3H^+ were formed. The polymerization exhibits a faster polymerization rate (monomer conversion >99.9% in 4 h), higher dispersity of PDMS ($Đ$ = 2.56), and significant difference between $M_{n,GPC}$ and $M_{n,th}$. Figure 2A,B depicts the ^{1}H NMR and GPC curves from the controlled experiments. In the ^{1}H NMR spectra, two signal peaks are observed at approximately 0.015 and 0 ppm for the polymerization products, which can be considered as cyclic oligomers resulting from side reactions and linear PDMS, respectively. The percentage of side reaction products is evidently higher in the $CF_3SO_3H^-$-catalyzed polymerization compared to that catalyzed by PAG2. The GPC curve for the $CF_3SO_3H^-$-catalyzed polymerization exhibits a distinct low molar mass shoulder peak attributed to the presence of linear PDMS oligomers and cyclosiloxanes resulting from side reactions. These experimental results reveal that ion pairs $PAG2^-$−D_3H^+ exhibit a higher degree of stability than the active species, leading to a decreased polymerization rate and fewer side reactions.

DFT calculations were employed to investigate the anisotropy of the induced current density (AICD), electrostatic potential (ESP), and intermolecular forces, aiming to elucidate the difference in binding strength between ion pairs $PAG2^-$−D_3H^+ and $CF_3SO_3^-$−D_3H^+. As shown in Figure 2C,

Table 2. Photomediated CROP of Different Cyclosiloxanes

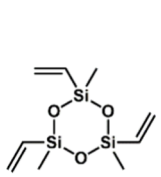

D_3^{Vi}

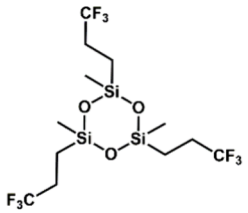

D_3^{TFPr}

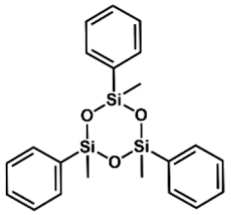

D_3^{Ph}

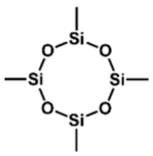

D_4^{H}

entry[a]	monomer	$[M]_0/[initiator]_0/[cat]_0$	time (h)	conversion (%)[b]	$M_{n,th}$[c]	$M_{n,GPC}$[d]	$Đ(M_w/M_n)$[d]
1	D_3^{Vi}	30/1/0.3	24	32.7	2658	3500	1.34
2	D_3^{TFPr}	30/1/0.3	24	49.7	7101	4300	1.29
3	D_3^{Ph}	10/1/0.5	24				
4	D_4^{H}	50/1/0.5	24	47.9	5870	3700	1.42

[a]Polymerization conditions: $[monomer]_0$ = 1.58 mol/L in toluene under blue light irradiation (460−465 nm, 8 W) at 30 °C using BnOH as the initiator and PAG2 as the catalyst. [b]Monomer conversions were calculated by ^{1}H NMR. [c]$M_{n,th} = [M]_0/[initiator]_0 \times conversion + M_{initiator}$. [d]Determined by GPC in toluene.

https://doi.org/10.1021/jacsau.4c00682
JACS Au 2024, 4, 4317−4327

paratropic ring current in the group of the benzene ring (a and c) and diatropic ring current in the group of oxygen-containing hexatomic ring (b) are observed in $PAG2^-$, indicating that the electrons in $PAG2^-$ exhibit strong delocalization and can move freely and quickly. Electron delocalization can change the distribution of the molecular electron cloud, thereby affecting the way or strength of its interaction with trisiloxonium ions. The ESPs of PAG2, CF_3SO_3H, and D_3 and their respective proton transfer products ($PAG2^-$, $CF_3SO_3^-$, and D_3H^+) are depicted in Figure 2D. For $PAG2^-$ and $CF_3SO_3^-$, the entire molecular region exhibits a negative potential with minimum electron ESPs of −125.5 and −128.4 kcal/mol, respectively, located at the $-SO_3^-$ position for both catalysts. In contrast, for D_3H^+, the entire molecular region displays a positive potential with a maximum electron ESP of 154.8 kcal/mol, situated at the $-OH^+$ position. This suggests that the $-SO_3^-$ group in $PAG2^-$ and $CF_3SO_3^-$ preferentially approaches the $-OH^+$ group in D_3H^+ by electrostatic attraction. The interaction energies (ΔE_{Int}) of ion pairs $PAG2^-$–D_3H^+ and $CF_3SO_3^-$–D_3H^+ were calculated via energy decomposition analysis, as shown in Figure 2E. The ΔE_{Int} values were determined by summing the contributions from electrostatic interaction energy (ΔE_{Els}), exchange-repulsion energy (ΔE_{Xrep}), orbital interaction energy (ΔE_{Orb}), and dispersive action energy (ΔE_{Disp}). The ΔE_{Int} value of $PAG2^-$–D_3H^+ (−116.51 kcal/mol) is lower than that of $CF_3SO_3^-$–D_3H^+ (−93.28 kcal/mol), confirming the superior stability and affinity between catalyst anions $PAG2^-$ and trisiloxonium ions D_3H^+.

Therefore, the polymerization conducted using PAG2 as the catalyst exhibits an enhanced control. Moreover, the degree of ion pair association between $PAG2^-$ and D_3H^+ is influenced by the solvent, with weaker binding forces observed in highly polar solvents compared to less polar ones. This elucidates why chloroform-mediated polymerization displays a faster reaction rate but inferior controllability compared to the cyclohexane- and toluene-involved polymerizations.

According to the experimental and calculation results, the proposed mechanism of photomediated CROP is illustrated in Figure 3. First, during the photoinduction process, isomeric transformation occurs to generate H^+ and $PAG2^-$. Subsequently, H^+ combines with D_3 to form trisiloxonium ions D_3H^+, and a short PDMS–OH chain is generated by a ring-opening reaction within the chain initiation process. Chain propagation proceeds through a consecutive ring-opening reaction between the resulting PDMS–OH and D_3. Although side reactions like intramolecular transfer (backbiting) and intermolecular chain transfer are not fully eliminated, their amount significantly decreases due to more stable active species, which enhances the controllability of polymerization.

Kinetic Study and Temporal Control

Kinetic analysis of photomediated CROP under different PAG2 loadings was performed, as depicted in Figure 4. The first-order linear semilogarithmic kinetic plots in Figure 4A indicate the presence of constant cationic active species, which can be attributed to the consistent hydrogen ion concentration and stable ion pairing. The number-average molar masses M_n increase linearly versus monomer conversions and agree well with the theoretical values (Figure 4B). As shown in Figure 4C, all resulting PDMS have low dispersities ($Đ$ < 1.30). The evolutions of ^{1}H NMR spectra are illustrated in Figure 4D, where methyl peaks in the monomer and polymer are located at approximately 0.08 and 0 ppm, respectively. A noticeable shift toward higher monomer conversion is observed. The GPC curves shown in Figure 4E are unimodal and shift toward higher molar mass regions with time. All these results confirm that the photomediated CROP using PAG2 as the catalyst is conducted in a controlled manner.

As expected from the mechanistic hypothesis, temporal control of polymer chain growth was demonstrated through intermittent exposure of the reactions to visible light, and the corresponding results are presented in Figure 5. The monomer conversion reaches 63.5% after 6 h of light irradiation, while the polymerization nearly ceases with a minimal change in monomer conversion (~64.1%) by turning off the light. The number-average molar mass M_n is almost unchanged during a 2 h dark period. This can be attributed to the rapid and reversible isomeric transformation of PAG2 under a light on/off switch, establishing a photocatalytic cycle between PAG2, D_3 monomer, and PDMS–OH chain. The on/off light switching cycle can be repeated to achieve higher monomer conversion and produce polymers with predetermined molar masses and low dispersities. The ^{1}H NMR spectra and GPC curves demonstrate a shift toward higher monomer conversion and an increased molar mass region corresponding to the duration of light irradiation. As expected from the mechanistic hypothesis, temporal control of polymer chain growth was demonstrated through intermittent exposure of the reactions to visible light.

In Situ Chain Extension

Chain-end fidelity of the resulting PDMS, prepared through photomediated CROP, was assessed by the in situ chain extension of D_3. Following 12 h of light irradiation during the initial polymerization process, the monomer conversion reaches 92.2%, yielding PDMS1 with a number-average molar mass (M_n) of 19,500 g/mol and a dispersity ($Đ$) of 1.24. A degassed mixture containing the D_3 monomer and toluene (2.5 mL, 1.58 M) was introduced using a nitrogen-purged syringe for the chain extension reaction. After 6 h of light irradiation, a successful chain-extended PDMS2 with M_n = 27,900 g/mol and $Đ$ = 1.31 was obtained, as evidenced by an obvious shift toward the higher molar mass region in the GPC traces (Figure 6).

Scope of Monomers

The photopolymerizations of other cyclosiloxanes, such as 1,3,5-trivinyl-1,3,5-trimethylcyclotrisiloxane (D_3^{Vi}), 1,3,5-trimethyl-1,3,5-tris(3,3,3-trifluoropropyl)cyclotrisiloxane (D_3^{TFPr}), 1,3,5-trimethyl-1,3,5-triphenylcyclotrisiloxane (D_3^{Ph}), and 2,4,6,8-tetramethylcyclotetrasiloxane (D_4^{H}), were conducted, respectively, in toluene using PAG2 as the catalyst and BnOH as the initiator. Successful initiation for the polymerizations of D_3^{Vi}, D_3^{TFPr}, and D_4^{H} was achieved (Table 2, entries 2, 3, and 5), producing polymers with low dispersities ($Đ$ < 1.50), confirming good applicability of photomediated CROP. However, no polymerization was observed for D_3^{Ph} because of a higher steric hindrance for benzyl in the monomer.

CONCLUSIONS

In summary, a newly designed merocyanine-based photoacid catalyst, 2-(3,5-di-*tert*-butyl-2-hydroxystyryl)-3,3-dimethyl-1-(3-sulfopropyl)-3H-indolium (PAG2), was synthesized as a catalyst for photomediated CROP. The polymerizations of D_3 under different catalyst loadings and initiator concentrations

https://doi.org/10.1021/jacsau.4c00682
JACS Au 2024, 4, 4317−4327

proceeded in a controlled manner, producing polymers with predetermined molar masses and low dispersities ($Đ$ < 1.30). Polymerizations in different solvents and various monomers were also conducted, producing well-defined polymers. The underlying mechanism of the controlled polymerizations was revealed by DFT calculations, which indicates that tight ion pairs between catalyst anions $PAG2^-$ and trisiloxonium ions are formed to form stable cationic active species to suppress intramolecular transfer (backbiting) and intermolecular chain transfer side reactions. Kinetic studies and in situ chain extension experiments further confirm the controlled characteristics of photomediated CROP. Good temporal control over the polymerization can be easily achieved by simply switching the light on and off because of the rapid and reversible isomeric transformation of a PAG2-enabled efficient photocatalytic cycle among PAG2, D_3 monomer, and PDMS−OH chain. In the future, the integration of this photocatalytic system with advanced polymer processing techniques can be tried to fabricate functional polymers with more complex structures and compositions, thus expanding application scenarios of organic silicon materials to such as electronics, biomedicine, and soft robotics. Also, development of photolatent catalysts enabling faster polymerization is ongoing for polyorganosiloxane synthesis.

■ ASSOCIATED CONTENT

Supporting Information

The Supporting Information is available free of charge at https://pubs.acs.org/doi/10.1021/jacsau.4c00682.

Reaction schemes, extra NMR spectra, GPC results, and DFT calculations (PDF)

■ AUTHOR INFORMATION

Corresponding Authors

Chao Bian − *School of Chemical Engineering, Shandong University of Technology, Zibo 255000, P. R. China;* orcid.org/0000-0002-8208-8792; Email: bianchao@sdut.edu.cn

Yin-Ning Zhou − *School of Chemistry and Chemical Engineering, Shanghai Jiao Tong University, Shanghai 200240, P. R. China;* orcid.org/0000-0003-3509-3983; Phone: +86-21-54745602; Email: zhouyn@sjtu.edu.cn; Fax: +86-21-54745602

Authors

Wenxu Zhang − *School of Chemical Engineering, Shandong University of Technology, Zibo 255000, P. R. China*

Shen Li − *School of Chemistry and Chemical Engineering, Shanghai Jiao Tong University, Shanghai 200240, P. R. China; School of Chemical Engineering and Technology, Hainan University, Haikou 570228, P. R. China*

Shuting Liu − *School of Chemical Engineering, Shandong University of Technology, Zibo 255000, P. R. China*

Tian-Tian Wang − *School of Chemistry and Chemical Engineering, Shanghai Jiao Tong University, Shanghai 200240, P. R. China;* orcid.org/0000-0002-4643-2357

Zheng-Hong Luo − *School of Chemistry and Chemical Engineering, Shanghai Jiao Tong University, Shanghai 200240, P. R. China;* orcid.org/0000-0001-9011-6020

Complete contact information is available at: https://pubs.acs.org/10.1021/jacsau.4c00682

Author Contributions

[‖]W.Z. and S.L. contributed equally to this work.

Notes

The authors declare no competing financial interest.

■ ACKNOWLEDGMENTS

The authors thank the National Natural Science Foundation of China (Nos. 22108160 and 22222807), Natural Science Foundation of Shandong Province (No. ZR2021QB026), and Postdoctoral Science Foundation of China (No. 2021M691962).

■ DEDICATION

This work is dedicated to the memory of Professor Yusuf Yagci.

■ REFERENCES

(1) Wolf, M. P.; Salieb-Beugelaar, G. B.; Hunziker, P. PDMS with designer functionalities-properties, modifications strategies, and applications. *Prog. Polym. Sci.* **2018**, *83*, 97−134.

(2) Wang, H.; Zhang, X.; Li, Y.; Xu, L. W. Siloxane-based organosilicon materials in electrochemical energy storage devices. *Angew. Chem., Int. Ed.* **2022**, *61*, No. e202210851.

(3) Li, S.; Zhang, J.; He, J.; Liu, W.; Wang, Y.; Huang, Z.; Pang, H.; Chen, Y. Functional PDMS elastomers: Bulk composites, surface engineering, and precision fabrication. *Adv. Sci.* **2023**, *10*, No. 2304506.

(4) Liu, Z.; Yang, Z.; Chen, X.; Tan, R.; Li, G.; Gan, Z.; Shao, Y.; He, J.; Zhang, Z.; Li, W.; Zhang, W. B. Discrete giant polymeric chains based on nanosized monomers. *JACS Au* **2020**, *1*, 79−86.

(5) Yilgör, E.; Yilgör, I. Silicone containing copolymers: Synthesis, properties and applications. *Prog. Polym. Sci.* **2014**, *39*, 1165−1195.

(6) Penczek, S.; Cypryk, M.; Duda, A.; Kubisa, P.; Słomkowski, S. Living ring-opening polymerizations of heterocyclic monomers. *Prog. Polym. Sci.* **2007**, *32*, 247−282.

(7) Köhler, T.; Gutacker, A.; Mejía, E. Industrial synthesis of reactive silicones: Reaction mechanisms and processes. *Org. Chem. Front.* **2020**, *7*, 4108−4120.

(8) Ganachaud, F.; Boileau, S.; Siloxane-Containing Polymers. In *Handbook of Ring-Opening Polymerization*, 2009, pp 65−95.

(9) Yactine, B.; Ratsimihety, A.; Ganachaud, F. Do-it-yourself functionalized silicones part 2: synthesis by ring opening polymerization of commercial cyclosiloxanes. *Polym. Adv. Technol.* **2010**, *21*, 139−149.

(10) Bezlepkina, K. A.; Milenin, S. A.; Vasilenko, N. G.; Muzafarov, A. M. Ring-opening polymerization (ROP) and catalytic rearrangement as a way to obtain siloxane mono-and telechelics, as well as well-organized branching centers: History and prospects. *Polymers* **2022**, *14*, 2408.

(11) Ottou, W. N.; Mondière, A. B.; Parisot, H.; Blanc, D.; Portinha, D.; Fleury, E. Imidazolium triflimide-based Brønsted acidic ionic liquid as organocatalyst to trigger the cationic ring-opening polymerization of cyclotrisiloxanes. *Polym. Chem.* **2023**, *14*, 4693−4703.

(12) Shi, J.; Zhao, N.; Xia, S.; Liu, S.; Li, Z. Phosphazene superbase catalyzed ring-opening polymerization of cyclotetrasiloxane toward copolysiloxanes with high diphenyl siloxane content. *Polym. Chem.* **2019**, *10*, 2126−2133.

(13) Shi, J.; Liu, Z.; Zhao, N.; Liu, S.; Li, Z. Controlled ring-opening polymerization of hexamethylcyclotrisiloxane catalyzed by trisphosphazene organobase to well-defined poly (dimethylsiloxane)s. *Macromolecules* **2022**, *55*, 2844−2853.

(14) Fuchise, K.; Igarashi, M.; Sato, K.; Shimada, S. Organocatalytic controlled/living ring-opening polymerization of cyclotrisiloxanes initiated by water with strong organic base catalysts. *Chem. Sci.* **2018**, *9*, 2879−2891.

(15) Fuchise, K.; Sato, K.; Igarashi, M. Precise synthesis of linear polysiloxanes end-functionalized with alkynylsilyl groups by organocatalytic ring-opening polymerization of cyclotrisiloxanes. *Macromolecules* **2021**, *54*, 5765−5773.
(16) Fuchise, K.; Sato, K.; Igarashi, M. Precise synthesis of side-chain-functionalized linear polysiloxanes by organocatalytic ring-opening polymerization of monofunctional cyclotrisiloxanes. *Macromolecules* **2021**, *54*, 5204−5217.
(17) Fuchise, K.; Kobayashi, T.; Sato, K.; Igarashi, M. Organocatalytic ring-opening polymerization of cyclotrisiloxanes using silanols as initiators for the precise synthesis of asymmetric linear polysiloxanes. *Polym. Chem.* **2020**, *11*, 7625−7636.
(18) Fuchise, K.; Sato, K.; Igarashi, M. Precise synthesis of linear polysiloxanes with a polar side-chain structure by organocatalytic controlled/living ring-opening polymerization of (3-cyanopropyl) pentamethylcyclotrisiloxane. *Polym. Chem.* **2021**, *12*, 3321−3331.
(19) Fuchise, K.; Sato, K.; Igarashi, M. Organocatalytic controlled/living ring-opening polymerization of 1, 3, 5-triphenyl-1, 3, 5-tri-p-tolylcyclotrisiloxane for the precise synthesis of fusible, soluble, functionalized, and solid poly [phenyl (p-tolyl) siloxane]s. *Polym. Chem.* **2021**, *12*, 5178−5190.
(20) Sato, K. I.; Ito, S.; Higashihara, T.; Fuchise, K. Precise synthesis of α, ω-chain-end functionalized poly (dimethylsiloxane) with azide groups based on metal-free ring-opening polymerization and a quantitative azidation reaction. *React. Funct. Polym.* **2021**, *166*, No. 105009.
(21) Toskas, G.; Besztercey, G.; Moreau, M.; Masure, M.; Sigwalt, P. Cationic polymerization of hexamethylcyclotrisiloxane by trifluoromethanesulfonic acid and its derivatives, 2. Reaction involving activated trifluoromethylsulfonates. *Macromol. Chem. Phys.* **1995**, *196*, 2715−2735.
(22) Wilczek, L.; Chojnowski, J. Acidolytic ring opening of cyclic siloxane and acetal monomers. Role of hydrogen bonding in cationic polymerization initiated with protonic acids. *Macromolecules* **1981**, *14*, 9−17.
(23) Chojnowski, J.; Mazurek, M.; Ščibiorek, M.; Wilczek, L. Cationic polymerization of siloxanes. Approach to the mechanistic studies. *Macromol. Chem. Phys.* **1974**, *175*, 3299−3303.
(24) Arraez, F. J.; Xu, X.; Edeleva, M.; Van Steenberge, P. H.; Marien, Y. W.; Jerca, V. V.; Hoogenboom, R.; D'hooge, D. R. Differences and similarities between mono-, bi- or tetrafunctional initiated cationic ring-opening polymerization of 2-oxazolines. *Polym. Chem.* **2022**, *13*, 861−876.
(25) Van Steenberge, P. H.; Sedlacek, O.; Hernández-Ortiz, J. C.; Verbraeken, B.; Reyniers, M. F.; Hoogenboom, R.; D'hooge, D. R. Visualization and design of the functional group distribution during statistical copolymerization. *Nat. Commun.* **2019**, *10*, 3641.
(26) Van Steenberge, P. H.; Verbraeken, B.; Reyniers, M. F.; Hoogenboom, R.; D'hooge, D. R. Model-based visualization and understanding of monomer sequence formation in gradient copoly(2-oxazoline)s on the basis of 2-methyl-2-oxazoline and 2-phenyl-2-oxazoline. *Macromolecules* **2015**, *48*, 7765−7773.
(27) Shi, L.; Boulegue-Mondiere, A.; Blanc, D.; Baceiredo, A.; Branchadell, V.; Kato, T. Ring-opening polymerization of cyclic oligosiloxanes without producing cyclic oligomers. *Science* **2023**, *381*, 1011−1014.
(28) Zhou, Y.-N.; Li, J.-J.; Wu, Y.-Y.; Luo, Z.-H. Role of external field in polymerization: Mechanism and kinetics. *Chem. Rev.* **2020**, *120*, 2950−3048.
(29) Doerr, A. M.; Burroughs, J. M.; Gitter, S. R.; Yang, X.; Boydston, A. J.; Long, B. K. Advances in polymerizations modulated by external stimuli. *ACS Catal.* **2020**, *10*, 14457−14515.
(30) Wang, Q.; Bai, F. Y.; Wang, Y.; Niu, F.; Zhang, Y.; Mi, Q.; Hu, K.; Pan, X. Photoinduced ion-pair inner-sphere electron transfer-reversible addition-fragmentation chain transfer polymerization. *J. Am. Chem. Soc.* **2022**, *144*, 19942−19952.
(31) Bian, C.; Zhou, Y.-N.; Guo, J.-K.; Luo, Z.-H. Aqueous metal-free atom transfer radical polymerization: Experiments and model-based approach for mechanistic understanding. *Macromolecules* **2018**, *51*, 2367−2376.
(32) Tasdelen, M. A.; Lalevée, J.; Yagci, Y. Photoinduced free radical promoted cationic polymerization 40 years after its discovery. *Polym. Chem.* **2020**, *11*, 1111−1121.
(33) Zhao, B.; Wilson, P. Recent progress and applications enabled via electrochemically triggered and controlled chain-growth polymerizations. *Polym. Chem.* **2023**, *14*, 2000−2021.
(34) Qi, M.; Dong, Q.; Wang, D.; Byers, J. A. Electrochemically switchable ring-opening polymerization of lactide and cyclohexene oxide. *J. Am. Chem. Soc.* **2018**, *140*, 5686−5690.
(35) Huang, Y.; Hu, C.; Pang, X.; Zhou, Y.; Duan, R.; Sun, Z.; Chen, X. Electrochemically controlled switchable copolymerization of lactide, carbon dioxide, and epoxides. *Angew. Chem., Int. Ed.* **2022**, *61*, No. e202202660.
(36) Lorandi, F.; Fantin, M.; Shanmugam, S.; Wang, Y.; Isse, A. A.; Gennaro, A.; Matyjaszewski, K. Toward electrochemically mediated reversible addition-fragmentation chain-transfer (eRAFT) polymerization: Can propagating radicals be efficiently electrogenerated from RAFT agents? *Macromolecules* **2019**, *52*, 1479−1488.
(37) D'hooge, D. R.; Fantin, M.; Magenau, A. J.; Konkolewicz, D.; Matyjaszewski, K. Two-compartment kinetic Monte Carlo modelling of electrochemically mediated ATRP. *React. Chem. Eng.* **2018**, *3*, 866−874.
(38) Kumar, A. R. S.; Padmakumar, A.; Kalita, U.; Samanta, S.; Baral, A.; Singha, N. K.; Ashokkumar, M.; Qiao, G. G. Ultrasonics in polymer science: Applications and challenges. *Prog. Mater. Sci.* **2023**, *136*, No. 101113.
(39) Price, G. J.; Lenz, E. J.; Ansell, C. W. G. The effect of high-intensity ultrasound on the ring-opening polymerisation of cyclic lactones. *Eur. Polym. J.* **2002**, *38*, 1753−1760.
(40) Wang, Y.; Bian, C.; Feng, W.; Yang, N. Ultrasonication enhanced photocatalytic solvent-free reversible deactivation radical polymerization up to high conversion with good control. *Eur. Polym. J.* **2022**, *168*, No. 111118.
(41) Wang, J.; Zhang, L.; Chen, D.; Wang, C.; Ren, Z.; Wang, Z. A mechanoredox catalyst facilitates atrp of vinylcyclopropanes. *Macromolecules* **2024**, *57*, 6267−6274.
(42) Aydogan, C.; Yilmaz, G.; Shegiwal, A.; Haddleton, D. M.; Yagci, Y. Photo-induced controlled/living polymerizations. *Angew. Chem., Int. Ed.* **2022**, *61*, No. e202117377.
(43) Dadashi-Silab, S.; Doran, S.; Yagci, Y. Photoinduced electron transfer reactions for macromolecular syntheses. *Chem. Rev.* **2016**, *116*, 10212−10275.
(44) Michaudel, Q.; Kottisch, V.; Fors, B. P. Cationic polymerization: From photoinitiation to photocontrol. *Angew. Chem., Int. Ed.* **2017**, *56*, 9670−9679.
(45) Sifri, R. J.; Ma, Y.; Fors, B. P. Photoredox Catalysis in Photocontrolled Cationic Polymerizations of Vinyl Ethers. *Acc. Chem. Res.* **2022**, *55* (14), 1960−1971.
(46) Corrigan, N.; Shanmugam, S.; Xu, J.; Boyer, C. Photocatalysis in organic and polymer synthesis. *Chem. Soc. Rev.* **2016**, *45*, 6165−6212.
(47) Shi, S.; Croutxé-Barghorn, C.; Allonas, X. Photoinitiating systems for cationic photopolymerization: Ongoing push toward long wavelengths and low light intensities. *Prog. Polym. Sci.* **2017**, *65*, 1−41.
(48) Coban, Z. G.; Kiliclar, H. C.; Yagci, Y. Photoinitiated cationic ring-opening polymerization of octamethylcyclotetrasiloxane. *Molecules* **2023**, *28*, 1299.
(49) Belfield, K. D.; Zhang, G. Photoinitiated cationic ring-opening polymerization of a cyclosiloxane. *Polym. Bull.* **1997**, *38*, 165−168.
(50) Fu, C.; Xu, J.; Boyer, C. Photoacid-mediated ring opening polymerization driven by visible light. *Chem. Commun.* **2016**, *52*, 7126−7129.
(51) Zivic, N.; Kuroishi, P. K.; Dumur, F.; Gigmes, D.; Dove, A. P.; Sardon, H. Recent advances and challenges in the design of organic photoacid and photobase generators for polymerizations. *Angew. Chem., Int. Ed.* **2019**, *58*, 10410−10422.

https://doi.org/10.1021/jacsau.4c00682
JACS Au 2024, 4, 4317−4327

(52) Weinhold, F.; West, R. The nature of the silicon-oxygen bond. *Organometallics* **2011**, *30*, 5815−5824.
(53) Kusumoto, S.; Nakagawa, T.; Yokoyama, Y. All-optical fine-tuning of absorption band of diarylethene with photochromic acid-generating spiropyran. *Adv. Opt. Mater.* **2016**, *4*, 1350−1353.
(54) Shi, Z.; Peng, P.; Strohecker, D.; Liao, Y. Long-lived photoacid based upon a photochromic reaction. *J. Am. Chem. Soc.* **2011**, *133*, 14699−14703.

https://doi.org/10.1021/jacsau.4c00682
JACS Au 2024, 4, 4317−4327